Heliyon 10 (2024) e38994

Contents lists available at ScienceDirect

Heliyon

journal homepage: www.cell.com/heliyon

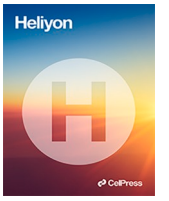

Research article

Amelioration of full-thickness cutaneous wound healing using stem cell exosome and zinc oxide nanoparticles in rats

Mohamed Salem [a,b], Ahmed Ateya [c], Zeinab Shouman [d], Basma Salama [e], Basma Hamed [f], Gaber Batiha [g], Farid Ataya [h], Athanasios Alexiou [i,j], Marios Papadakis, Corresponding [k,**], Marwa Abass [a,*]

[a] Department of Surgery, Anesthesiology, and Radiology, Faculty of Veterinary Medicine, Mansoura University, Mansoura, 35516, Egypt
[b] Department of Veterinary Clinical Sciences, Faculty of Veterinary Medicine, Jordan University of Science and Technology, Irbid, 22110, Jordan
[c] Department of Development of Animal Wealth, Faculty of Veterinary Medicine, Mansoura University, Mansoura, 35516, Egypt
[d] Department of Cytology and Histology, Faculty of Veterinary Medicine, Mansoura University, Mansoura, 35516, Egypt
[e] Department of Biochemistry and Molecular Biology, Faculty of Veterinary Medicine, Mansoura University, Mansoura, 35516, Egypt
[f] Mansoura experimental research center (MERC), Faculty of Medicine, Mansoura, 35516, Egypt
[g] Department of Pharmacology and Therapeutics, Faculty of Veterinary Medicine, Damanhour University, Damanhour 22511, AlBeheira, Egypt
[h] Department of Biochemistry, College of Science, King Saud University, PO Box 2455, Riyadh, 11451, Saudi Arabia
[i] Department of Research & Development, Funogen, Athens, 11741, Greece
[j] University Centre for Research & Development, Chandigarh University, Chandigarh-Ludhiana Highway, Mohali, Punjab, India
[k] Department of Surgery II, University Hospital Witten-Herdecke, Heusnerstrasse 40, University of Witten-Herdecke, 42283, Wuppertal, Germany

ARTICLE INFO

Keywords:
Exosome
Zinc nanoparticles
Skin wound
Rats
Gene expression

ABSTRACT

Background: Wound healing is a complex procedure that requires the coordination of several factors, so this study aimed to assess the zinc oxide nanoparticles' regenerated effect and stem cell exosomes on full-thickness wounds in rats.

Methods: Seventy-two Wistar male rats were subjected to a full-thickness skin defect (20 mm2) on the dorsal surface of each rat between two shoulder joints. The rats were randomized into four groups (18/group) according to wound treatments. The wounds were irrigated with normal saline (Control group), or the wound's edges were subcutaneously injected daily with 0.3 ml of exosome (Exo-group), or 1 ml of zinc oxide nanoparticles (ZnO2-NPs group), or 0.3 ml of exosome in combined with 1 ml of zinc oxide nanoparticles (Exo/ZnO2-NPs group). On the 7th, 14th, and 21st days post-wounding, the weight of the rats, the wound healing breaking strength, the wound size, and the contraction percent were evaluated. Six rats in each group were euthanized at each time point for histopathological, immunohistochemical examination of collagen, the levels of alpha-smooth muscle actin (α-SMA), and epidermal growth factor receptor (EGFR). additionally, the gene expression analysis of the relative renal nuclear factor erythroid 2-related factor2 (Nrf2 mRNA), Transforming growth factor beta-1 (TGFβ1), fibroblast growth factor-7 (FGF7), Transforming growth factor beta-1 (TGFβ1), Lysyl oxidase (LOX), and Vascular endothelial growth factor (VEGF) were applied.

* Corresponding author. Department of Surgery, Anesthesiology, and Radiology, Faculty of Veterinary Medicine, Mansoura University, Mansoura, 35516, Egypt.

** Corresponding author. Department of Surgery II, University Hospital Witten-Herdecke, Heusnerstrasse 40, University of Witten-Herdecke, 42283, Wuppertal, Germany.

E-mail addresses: Marios.Papadakis@uni-wh.de, drmariospapadakis@gmail.com (M. Papadakis), marwa_mossa@mans.edu.eg (M. Abass).

https://doi.org/10.1016/j.heliyon.2024.e38994
Received 24 June 2024; Received in revised form 28 September 2024; Accepted 4 October 2024
Available online 5 October 2024

Results: The Exo-group exhibited a significant decrease in wound size and a significant increase in wound contraction compared with other groups. Histopathologically evaluation during the three intervals revealed that the Exo-group had the highest collagen deposition area with a significant reduction of the granulation tissue. Moreover, upregulated gene expression profiles of the growth factors genes at all time points post-wounding.
Discussion: The exosomes-treated group revealed superior wound healing and contraction, with minimal inflammatory signs, higher angiogenesis, and myofibroblasts, and associated with higher growth factor expression genes compared to the other groups.
Conclusions: Exosome-based therapy demonstrates potential as a treatment method to promote and accelerate wound healing by modulating angiogenesis, re-epithelialization, collagen deposition, and gene expression profiles.

1. Introduction

The skin is a complex barrier that separates the body from the external environment. It has multiple layers and performs various functions, such as regulating body temperature, protecting against pathogens, preventing dehydration, and facilitating the sensation and transportation of water [1–3]. The skin can be ruptured and change its anatomy and physiology, resulting in a wound due to factors such as biological, thermal, physical, and chemical causes. Wound healing is an intricate process of restoring cells that have been damaged to their original state through re-epithelialization, in addition to tensile strength [4]. The wound-healing process encompasses various biological as well as molecular events, including proliferation, cellular migration, and extracellular matrix (ECM) deposition at the injury site [5,6].

In recent times, nanotechnology has acquired significant significance owing to its capacity to transform metals into their nanoscale form, thereby profoundly altering their optical, physical, and chemical characteristics [7]. Zinc is an essential element that plays a crucial role in many cellular activities. It acts as a cofactor in both catalytic and structural reactions in microorganisms and higher organisms [8,9]. Zinc oxide nanoparticles (ZnO_2-NPs) possess unique electromagnetic and optical characteristics, making them highly

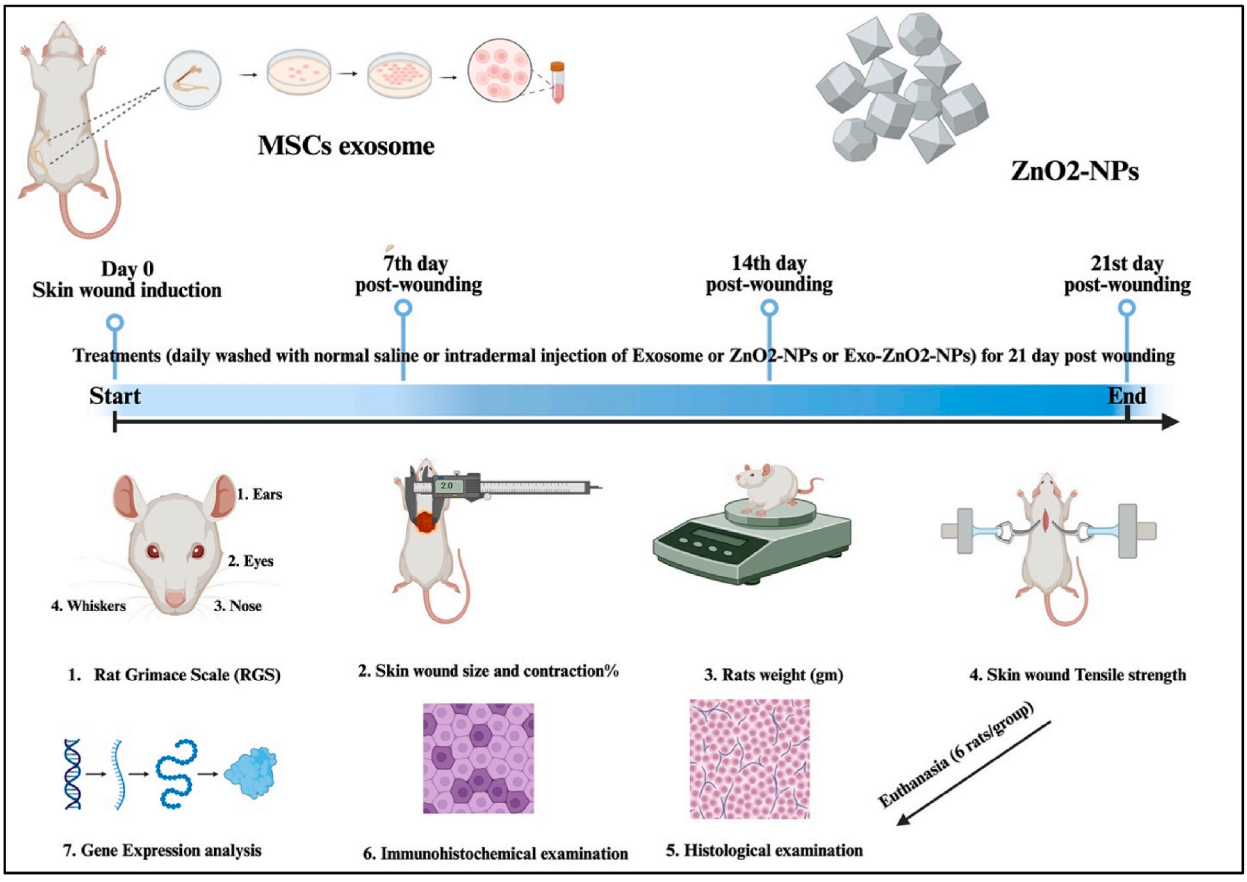

Scheme 1. The schematic illustration of this experimental strategy. (Created with Biorender.com with permission).

suitable for a range of biomedical applications, including targeted drug delivery, imaging techniques, and sensors in biological systems [10,11]. ZnO_2-NPs have been documented to exhibit anti-inflammatory, antifungal, and antibacterial activities. Additionally, they facilitate the wound healing process by promoting the growth of fibroblast cells and angiogenesis at the wound site. As a result, they are combined with various agents used for managing dermal wounds [12]. Applying zinc directly to a wound is more effective than oral administration due to its potent capacity to alleviate superinfections, inflammation, and necrotic components via activating collagenolysis, re-epithelialization, and local defense systems [13].

Exosomes are a type of extracellular vehicle (EVs) (30–150 nm) in diameter. Their composition includes DNA, proteins, RNA, and lipids. Exosomes transfer their contents to the target cells' cytoplasm, resulting in a change in the recipient cells' physiological state. Exosomes have been proven to be participants in intercellular communication. Research has also demonstrated that exosomes can serve as biomarkers to diagnose diseases, along with predicting prognosis [14]. Exosome secretion occurs via different cell types, such as mesenchymal stem cells (MSCs) [15], microglia [16], immune cells [17], and cancer cells [18].

Exosomes derived from various sources can regulate the activity of cells that are implicated in the wound healing process. They facilitate neovascular growth [19], enhance collagen deposition [20], and suppress inflammation [21], contributing to wound healing acceleration. Furthermore, suppressing the highly expressed microRNAs (miRNAs) in exosomes can partially mitigate the challenges associated with healing diabetic wounds [22]. The objective of this study was to investigate the regenerative efficacy of stem cell exosomes and ZnO_2-NPs in the healing of full-thickness cutaneous wounds in rats through macroscopic evolution, and microscopy of the wound healing process. This study tested the hypothesis that stem cell exosomes combined with ZnO_2-NPs induced promote rat cutaneous wound healing.

2. Materials and methods

2.1. Animals

The experiment involved seventy-two male, Wistar rats weighing 250 ± 15.23 gm, aged 16 ± 2 weeks obtained from the Medical Experimental Research Center of Mansoura University (MERC). They were maintained in regular polypropylene cages (four rats per cage), under illumination cycles (14 h illuminated and 10 h darkness) in a temperature-controlled environment at 20 °C. Rats fed on a standard diet with no restriction of water. Male rats were chosen to minimize variation as they do not affect the hormonal cycle of the cell response. This study was approved by the Mansoura University Animal Care and Use Committee (MU-ACUC) with the code number (VM.R.24.10.181; Scheme 1). All procedures were reported following the format specified by ARRIVE [23].

G- Power 3.1.9.4 software was used to determine the minimum sample size required to test the study hypothesis. Results indicated the required sample size to achieve 95 % power for detecting a medium effect, at a significance criterion of $\alpha = 0.05$, with an effect size $f = 0.5$, and critical F-value = 3.336, was N = 12 for [A repeated measure ANOVA]. Thus, the sample size of N = 72 is adequate to test the study hypothesis.

2.1.1. Mesenchymal stem cell exosome preparation

2.1.1.1. Bone marrow (BM) harvesting. Sacrificing of healthy female adults, Sprague Dawley rats was done utilizing cervical dislocation. The skin was subsequently sterilized with ethyl alcohol (70 %) before making an incision in the skin. Dissection of the tibia and femurs was carefully done (from adherent soft tissues). Afterward, they were transferred to a sanitized beaker filled with a solution of ethyl alcohol (70 %) for a duration of 1–2 min. The bones were placed in a Petri dish filled with phosphate-buffered saline (PBS) solution for rinsing *according to* Refs. [24,25]. The bones were transported to a laminar airflow to obtain the BM. The sterile scissors were utilized to separate the two ends of the bones. At one end, bones were washed with complete media (3–5 ml). The marrow plugs were ejected from the opposing extremity of the bone into a sterile tube (15 ml). Marrow plug incubation was done utilizing complete media (15 ml).

2.1.2. Culturing of bone marrow- mesenchymal stem cells (BM-MSCs)

The cells were cultured in a tissue culture flask (75 cm^2) containing a complete media medium (10–15 ml) that contains Dulbecco's Modified Eagle Medium (DMEM) supplemented with 10 % fetal bovine serum (DMEM-FBS), 100 μg/ml streptomycin, 1 % nonessential amino acids, 100 IU/ml penicillin, and 1 % L-glutamine. Cell incubation was done in a humidified incubator at 37 °C with 5 % carbon dioxide (CO_2). Examination of cultured cells was done daily, utilizing the inverted microscope to follow up on cell growth. Following 24h, old media removal was done by aspiration utilizing a sterile pipette. Subsequently, cell wash was done utilizing 5 ml PBS. Fifteen milliliters of complete media were then introduced into the flask. MSCs were identified as different from other cells found in bone marrow due to their capacity to attach to a flask made of tissue culture polystyrene. The second media exchange took place approximately 3–4 days later. The media was changed biweekly. The MSCs were left to proliferate until reaching passage.

2.1.3. Harvesting of MSC exosome

MSCs from passage 3 were cultured in a serum-free medium containing DMEM supplemented with 1 % nonessential amino acids, 100 IU/ml penicillin, 1 % L-glutamine, and 100 μg/ml streptomycin, and incubated with 5 % CO2 at 37 °C for 24 h. After 24-h incubation, the media were collected and referred to as conditioned media (CM). These media contain exosomes from MSCs and were pooled. The CM was subjected to differential ultracentrifugation at 4 °C to eliminate any dead cells or cellular debris. Following the

initial centrifugation, the cm underwent ultracentrifugation at 1,000,000×*g* for 90 min to facilitate the formation of exosome precipitates **(**Fig. 1A and B**).** The precipitated exosomes were subjected to two washes with PBS and then resuspended in PBS. They were maintained at a temperature of −80 °C under sterile conditions in aliquots.

2.2. Zinc oxide nanoparticles (ZnO_2-NPs)

ZnO_2-NPs dispersion with 20 wt% concentration in H_2O was purchased from Sigma-Aldrich Chemicals No (Nasr City-Cairo-Egypt) and stored in a dark room at ambient temperature. It contains ZnO_2-NPs (100 g) in the form of milky white color dispersion (in a dark glass bottle) (Fig. 2A, B). The dispersion of ZnO_2-NPs was diluted to a concentration of 0.2 % utilizing a solution of 0.9 % normal saline [26].

2.3. Induction of the wounds

Anesthesia was induced through intramuscular administration of xylazine HCL (20 mg/ml, Xylaject-ADWIA-Cairo-Egypt) at a dosage of (4 mg/kg), ketamine HCL (50 mg/ml, Aneket®-NEON Laboratories Ltd-Mumbai-India) at a dosage of 0.5 mg/kg, and butorphanol (2 mg/ml, Alvegesic-CP. Pharma-Germany). Following this, the hair was removed from the dorsal surface of the rat's back. A 20 mm^2 full-thickness skin defect was made by skin removal from each rat's dorsal surface. Rats received intramuscular injection utilizing a single meloxicam dose (0.3 mg/kg) for analgesic effects.

Post-wounding, the rats were kept in individual regular polypropylene cages at room temperature with free access to commercial feed and drinking water. Rats were randomized using the opaque sealed envelopes (SNOSE) method [27] into four groups (n = 18 per group). In the control group (C-group) wound irrigation was done utilizing 5 ml of normal saline (0.9 % sodium chloride solution, 500 ml, Ultimate Pharma-Egypt). In the Exo-group, the wound was treated with a daily SC injection of 0.3 ml of exosome at its edges. In the ZnO_2-NPs group, the wound was treated with a daily SC injection of 1 ml zinc oxide nanoparticle solution at its edges. In the Exo/ZnO_2-NPs group, the wound was treated with daily injections with 0.3 ml exosome and 1 ml of zinc nanoparticles at its edges. The rats were returned to individual cages. The wound was recorded photographically at the 7^{th}, 14^{th}, and 21^{st} days post-wounding. Six rats in each group were euthanized at the 7^{th}, 14^{th}, and 21^{st} days post-wounding for histopathological, immunohistochemical examination, and gene expression.

2.4. Macroscopic evaluation of wounds

The weight of the rats (gm) at baseline (before procedures) and on the 7^{th}, 14^{th}, and 21^{st} days post-wounding was recorded.

According to Ref. [28] the rat facial grimace scale (RGS) was scored at baseline (before procedures) and on the 7^{th}, 14^{th}, and 21^{st} days post-wounding s and RGS.

Any expected or unexpected adverse events including stress, pain signs, or infection of the wound were recorded. A digital camera captured images of wounds on the infliction day (Day 0) as well as on the 7^{th}, 14^{th}, and 21^{st} days post-wounding. Moreover, a digital caliper was utilized to assess and determine the dimensions of wounds in the four groups. The wound contraction area percentage calculation was determined utilizing the equation as follows: wound contraction % = 1- (Ad\A0) × 100. The variables A0 and Ad were utilized to measure the size of the wound on day zero and on subsequent days to assess the progress of wound healing and determine its effectiveness, as previously indicated. An expert who was blinded to the study procedures reported wounds' visual observation.

2.5. Tensile strength and breaking strength measurements

On the 7^{th}, 14^{th}, and 21^{st} post-wounding, the rats were anesthetized and secured on the operating table. A line was drawn 3 mm

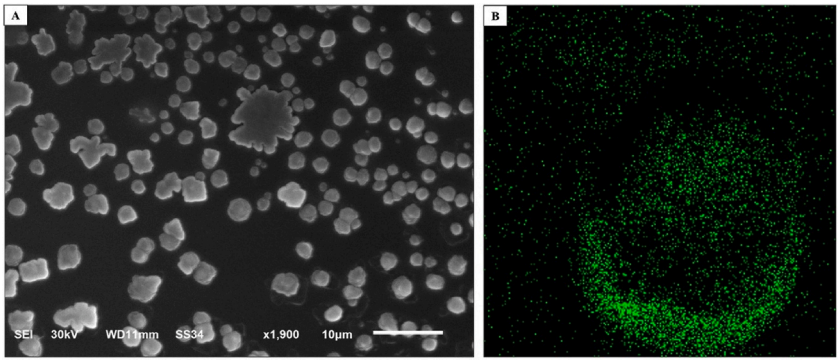

Fig. 1. Identification of bone marrow mesenchymal stem cell-derived exosomes (BMSC-Exos) and BMSC-Exos uptake by macrophages in vitro. (A) Representative transmission electron microscopy (TEM) image of Exosome 1,900X and 10 μm. (B) The Energy Dispersive X-ray (EDX) mapping addressed the Exosome.

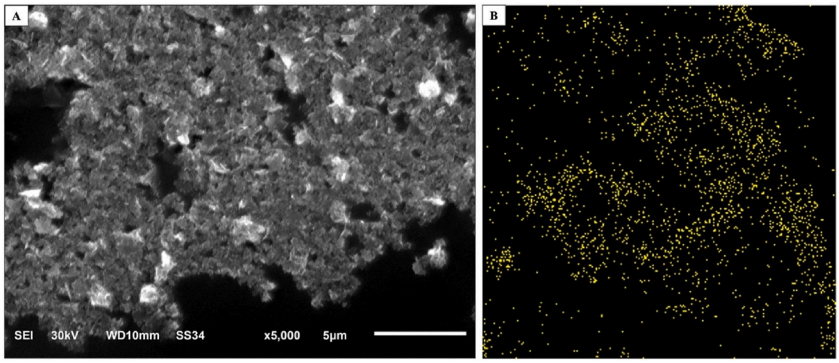

Fig. 2. Scanning electron microscopy (SEM) of Zinc Oxide nanoparticles detects the morphology of ZnO_2 at 5000X (A). EDX mapping of addressed Zinc Oxide nanoparticles (B).

away from each side of the wound. The lines were clamped with two forceps, with the ends of the forceps opposite each other. One side of the forceps was connected to a freely suspended weight (gm) through a string that ran over a pulley. The weight was recorded when the wound first opened up. The average of three different recorded readings for the incision wounds was taken as an individual value of breaking strength [29]**.** Tensile strength was also calculated using the following formula: Tensile strength (gm/mm^2) = breaking strength (gm)/wound area of skin (mm^2).

2.6. Histological evaluation of the wounds

On days 7, 14, and 21 after wound creation, Skin fragments were collected and fixed in 10 % neutral buffered formalin. After 6 h, tissues were cleaved in half using a razor and kept in a fixation solution for 24 h. Routine procedures for processing paraffin embedding tissues were carried out, including dehydration, clearing, and embedding. Sectioning of paraffin-embedded tissue was done by microtome to obtain sections at a thickness of 4 μm and collect the sectioned tissue with a clean and identified glass slide. Afterward, Hematoxylin & Eosin (H&E) [30] and Masson's trichrome staining (to ascertain the collagen's maturity level) were performed [31].

The levels of alpha-smooth muscle actin (α-SMA) and epidermal growth factor receptor (EGFR) were determined using immunohistochemistry analysis. Following the process of rehydrating and removing paraffin from the skin samples using xylene, antigen retrieval was performed by subjecting the samples to boiling in a sodium citrate buffer with a pH of 6.0. The tissue sections were then exposed to primary antibodies for an extended time at a temperature of 4 °C. This was followed by a 1-h incubation with a secondary antibody that was conjugated to horseradish peroxidase. Subsequently, a DAB immunohistochemistry imaging kit was utilized to examine the samples. The stained section photographs were captured using a microscope [32].

2.7. Morphological analysis

Morphological analysis was carried out utilizing Image J software (version 1.32J) to evaluate the healing events according to specific parameters previously discussed [33]. Six fields per slide (3 slides/group) were evaluated to encompass the borders and the center of the wound. H&E-stained sections were utilized to detect the area of scab and granulation tissue (GT), while collagen deposition area was detected by analyzing Masson's trichrome-stained sections. Furthermore, vascularization and epithelialization were measured by examining immunohistochemically stained sections (α-SMA and EGFR, respectively).

2.8. Gene expression

2.8.1. Tissue sampling

Samples were dissected from each rat, which was then promptly frozen (in liquid nitrogen) and preserved at −80 °C. These samples were utilized for total RNA extraction and subsequent molecular gene expression analysis.

2.8.2. RNA extraction and reverse transcription

Trizol reagent was utilized for total RNA isolation based on the manufacturer's instructions (Direct-zolTM RNA MiniPrep, catalog No. R2050). The quantity and purity were determined utilizing a nanodrop (UV–Vis spectrophotometer Q5000/USA), and the integrity was assessed using gel electrophoresis. Subsequently, reaction mixture preparation was done in 20 μL total volume consisting of 1 μL reverse transcriptase, 4 μL 5x Trans Amp buffer, total RNA up to 1 μg, and DNase free-water up to 20 μL. The final reaction mixture was transferred to a thermal cycler and subjected to the following program: primer annealing at 25 °C for 10 min, reverse transcription at 42 °C for 15 min, and subsequent inactivation at 85 °C for 5 min. The samples were stored at 4 °C.

2.8.3. Quantitative real-time PCR

The fibroblast growth factor-7 (FGF7), vascular endothelial growth factor (VEGF), lysyl oxidase (LOX), bcl-2 Associated X-protein

(BAX), transforming growth factor beta-1 (TGFβ1), and the relative renal nuclear factor erythroid 2-related factor2 (Nrf2 mRNA) abundance were assessed via real-time PCR utilizing SYBR Green PCR Master Mix (2x SensiFast™ SYBR-Bioline-catalog No. Bio-98002). Moreover, the qRT-PCR analysis primer sequence. The housekeeping gene (β-Actin) was utilized as an internal control. Following that, the reaction mixture was performed in 20 μL total volume consisting of 5.4 μl H_2O (d.d water), 3 μL cDNA, 10 μL 2x SensiFast SYBR, and 0.8 μl of each primer. Real-time PCR conditions were performed as follows: 95 °C for 4 min followed by 40 cycles of 94 °C for 15 s, annealing temperatures for 30 s, and extension temperature at 72 °C for 20 s. Following the amplification phase, a melting curve analysis was conducted to verify the PCR product's specificity. To standardize gene expression levels in the target, the ratio of the gene's expression in each sample compared to controls, relative to the β-Actin gene, was determined using the 2-ΔΔCt method [34] as shown in Table 1.

2.9. Statistical analysis

Data collection and statistical analysis were performed utilizing the 16th version of the SPSS software. The Kolmogorov–Smirnov test was utilized to validate data distribution normality. The normally distributed numerical data were presented as mean and standard deviation. The unpaired *t*-test and ANOVA were utilized to statistically compare between groups followed by followed by Tukey-Kramer post-hoc test. All data were considered statistically significant if the p-value was ≤ 0.05.

3. Results

3.1. Macroscopic examination

Neither the weight of the rats nor the rat facial grimace scale showed any significant differences between groups or within the same group at different time points.

The Exo-group exhibited a notable reduction in wound size compared to the other groups. At each recorded time point, the Exo-group exhibited a reduced wound area that contracted swiftly in contrast to the other groups. The wounds in the Exo-group were closed approximately 21st days post-wounding, as shown in (Fig. 3).

The extent of wound healing over the specified time intervals is demonstrated in (Fig. 4). The Exo-group exhibited a substantial reduction in the diameter of the wound area (cm^2) at various measured time points ($p \leq 0.05$).

In addition, the Exo-group exhibited superior wound contraction percent compared to the other groups (Fig. 5). The macroscopic examination of the skin demonstrated the presence of skin inflammation in the group that was exposed to the ZnO_2-NPs group. The skin inflammation initially presented as mild erythema and edema. Subsequently, the back skin thickened, demonstrating crusting formation, ulceration, erosions, hemorrhage, and severe erythema.

3.2. Tensile strength measurement

The tensile strength measures of the Exo-treated rats were significantly higher on the 7th, 14th, and 21st day post-wounding than that of the other groups ($p < 0.01$) measuring 3.99 ± 3.1, 4.05 ± 2.3, and 4.25 ± 7.8 gm/mm^2 respectively. In comparison, the C-group had a tensile strength of 2.44 ± 1.3, 2.65, ±4.1and 2.84 ± 1.9 gm/mm^2 respectively, the ZnO_2-NPs group had a tensile strength of 2.87 ± 1.2, 2.91 ± 2.6, and 3.01 ± 1.7 gm/mm^2 respectively, and the Exo/ZnO_2-NPs group had a tensile strength of 2.95 ± 2.6, 3.16 ± 4.16, and 3.22 ± 3.4 gm/mm^2 respectively.

On the same side, the breaking strength values on the 7th, 14th, and 21st day post-wounding of Exo-treated rats were 727 ± 11.57, 777 ± 42.24, and 810 ± 21.81 gm respectively which increased significantly ($p < 0.02$) compared to the other groups. The breaking strength measures of the C-group were 488 ± 20.22, 520.3 ± 31.12, and 550 ± 10.37 gm respectively, whereas, in the ZnO_2-NPs group were 575 ± 17.60, 585.9 ± 23.40, and 596 ± 8.11 gm respectively, and the Exo/ZnO_2-NPs group were 639 ± 21.11, 660 ± 13.78, and

Table 1
Primers used for real-time PCR amplifications.

Gene	Gen Bank accession number	Oligonucleotide sequence	Annealing temperature (^{0}C)	Size (bp)	Source
FGF7	NM_022182.1	f5,- ACAGATAGGAGGAGGCCCAT -3, r5,- GGTGGAAGCACGGTCTGTAG -3,	59	156	Current study
VEGF	AY033508.1	f5,- GCAATGATGAAGCCCTGGAGT -3, r5,- GGAGACTGCCCATTCTCGAC -3,	60	249	Current study
LOX	NM_001414003.1	f5,- GCTACACAGGACATCACGCC -3, r5,- CACCAGGTACTGCTTCATCCTT -3,	60	93	Current study
BAX	U32098.1	f5, - GGAGACACCTGAGCTGACCTT-3, r5, - GTTGTTGTCCAGTTCATCGCCA-3,	60	100	Current study
TGFβ1	NM_021578.2	f5,- AGGGCTACCATGCCAACTTC-3, r5, -CCACGTAGTAGACGATGGGC-3,	59	168	Current study
Nrf2	NM_031144.3	f5, - GTCCACCCGCGAGTACAACCT-3, r5, - GGAGCCGTTGTCGACGACGA-3,	60	119	Current study
β-Actin	NM_031144.3	f5- GGCATGTGCAAGGCCGGCTT -3, r5,- TAGGAGTCCTTCTGACCCATA -3,	58	116	Current study

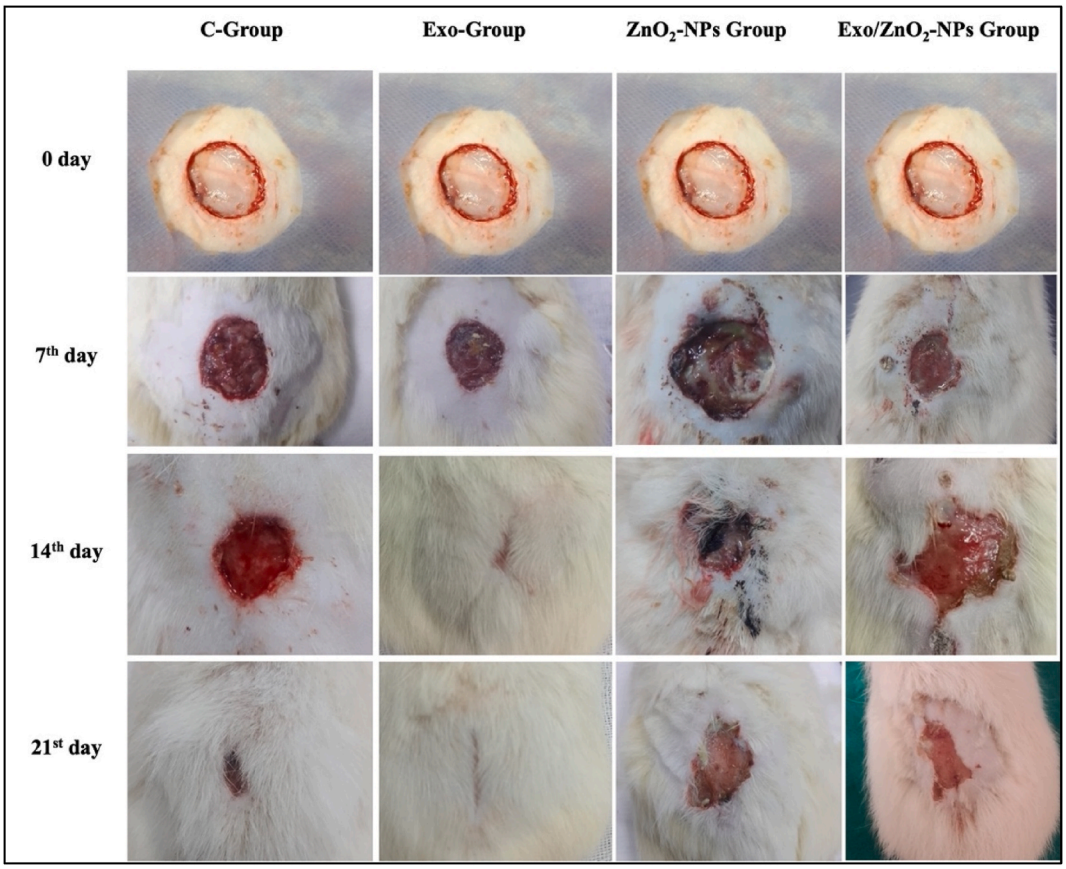

Fig. 3. The Macroscopic evaluation of the wound on the 7th, 14th, and 21st days post-wounding in the control group (C-group), exosome-treated group (Exo-group), zinc oxide nanoparticles group (ZnO_2-NPs group) and exosome/zinc oxide nanoparticles combination group (Exo/ZnO_2-NPs group).

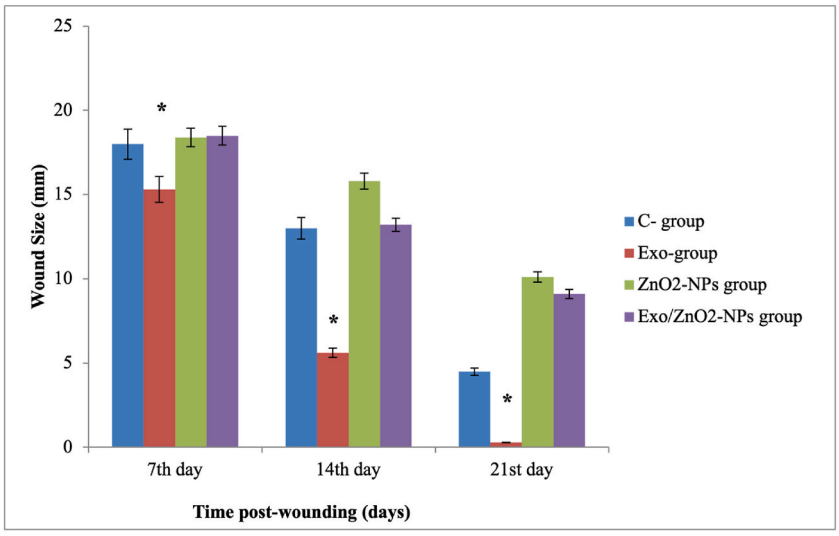

Fig. 4. The wound size measurements (mm) between the control (C-group), exosome-treated (Exo-group), zinc nanoparticles treated (ZNO_2-NPs group), and the combination between exosome and zinc nanoparticles treated groups (Exo/ZNO_2-NPs group) on the 7th, 14th, and 21st days post-wounding.

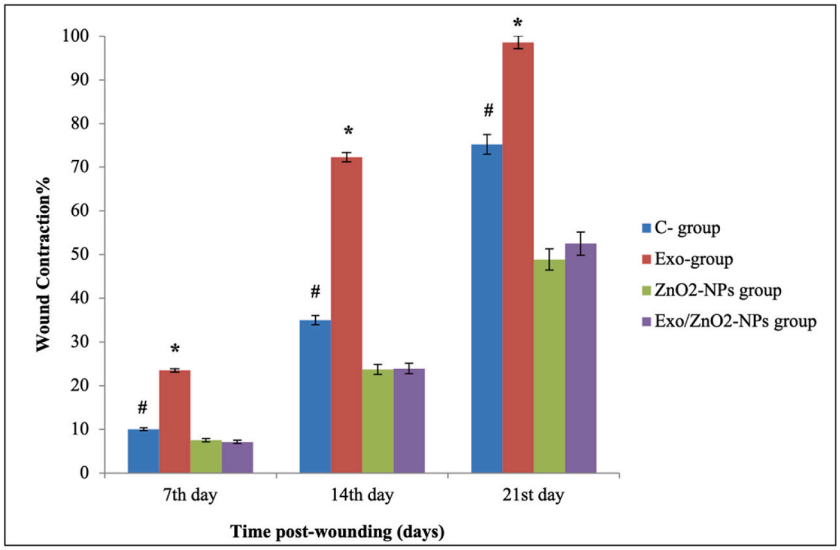

Fig. 5. The wound contraction percentage (%) between the control (C-group), exosome-treated (Exo-group), zinc nanoparticles treated (ZNO_2-NPs group), and the combination between exosome and zinc nanoparticles treated groups (Exo/ZNO_2-NPs group) on the 7th, 14th, and 21st days post-wounding.

673 ± 27.13 gm respectively (Fig. 6).

3.3. Histopathological and immunohistochemical study

3.3.1. Morphological analysis of wound area

On the seventh day, histological sections stained with H&E revealed that the wound area exhibited a granulation tissue (GT) covered by a scab. The group treated with ZnO_2-NPs, as well as the Exo/ZnO_2-NPs groups, exhibited a greater amount of the GT and a

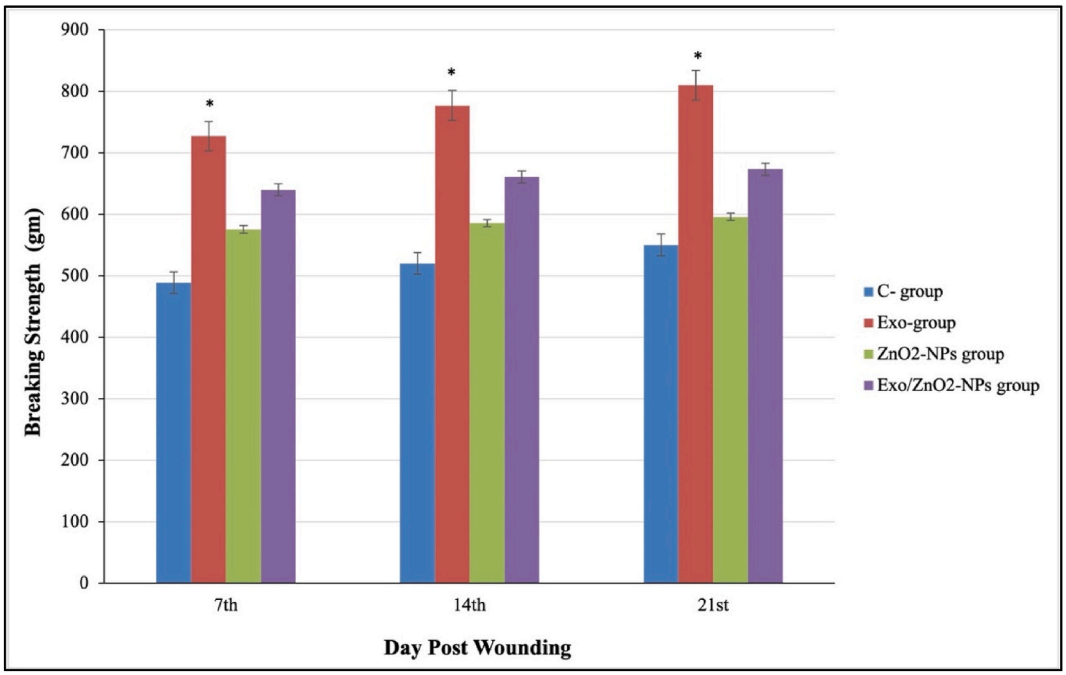

Fig. 6. The breaking strength measure (gm) of the healing skin wound in the control (C-group), exosome-treated (Exo-group), zinc nanoparticles treated (ZNO_2-NPs group), and the combination between exosome and zinc nanoparticles treated groups (Exo/ZNO_2-NPs group) on the 7th, 14th, and 21st days post-wounding.

larger scab compared to the other groups (Fig. 7a–d). On the 14th day, histological sections stained with H&E revealed reduced GT and a smaller scab in the wound area (Fig. 7e–h). Moreover, on the 21st day, the Exo-group exhibited a more advanced stage of healing and demonstrated complete closure of the wound, in contrast to the other groups that displayed reduced GT and smaller scabs (Fig. 7i–l and Fig. 9a and b).

Collagen Deposition (Masson's trichrome staining) is an important aspect of wound healing, as it provides structural support to the newly formed tissue. The analysis of Masson's trichrome-stained sections revealed that the control and ZnO_2-NPs groups had the lowest collagen deposition area while (Fig. 8a–e, i, c, g, k, and Fig. 9 c), the Exo/ZnO_2-NPs group showed the second-highest collagen deposition (Fig. 8d–h, l, and Fig. 9c). The Exo-group exhibited the highest collagen deposition area at all three-time intervals (Fig. 8b–f, j, and 9c). In addition, the number of alpha-smooth muscle actin (α-SMA) vessels/field, and % of epidermal growth factor receptors (EGFR) were significantly higher in the Exo-group compared to other treatments (Fig. 9d and e).

Immunohistochemical stained sections against α-SMA marker were analyzed. The positively reacted vessels were counted/field, and the result was significantly decreased, with the Exo-group consistently having the highest count among all groups at all three intervals (Fig. 10b–f, j). The Exo/ZnO_2-NPs groups (Fig. 10d–h, l) showed the second-highest vessel count, followed by the control group (Fig. 10a–e, i). The ZnO_2-NPs group had the lowest number of vessels (Fig. 10c–g, k). Furthermore, immunohistochemically stained sections against the EGFR marker were examined. The Exo-group showed the highest expression compared to other groups during the three intervals (Fig. 11b–f, j), control groups (Fig. 11a–e, i), and Exo/ZnO_2-NPs groups showed a lower expression (Fig. 11d–h, l). Meanwhile, the ZnO_2-NPs groups had the lowest expression (Fig. 11c–g, k). This result indicates enhanced re-epithelialization.

3.4. Gene expression

The rats in the Exo-group showed upregulate the expression profile of FGF7, VEGF, LOX, TGFβ1, and Nrf2 genes at 7, 14, and 21 days compared to the C-, ZnO_2-NPs, and Exo/ZnO_2-NPs groups. However, the mRNA level of the BAX marker was downregulated. In addition, the Exo/ZnO_2-NPs group exhibited a significant down-regulation of FGF7, VEGF, LOX, TGFβ1, and Nrf2 compared to controls. In contrast, the BAX gene was upregulated (Fig. 12).

4. Discussion

The clinical examination of the group treated with exosomes revealed superior wound healing and contraction, with minimal inflammation compared to the other groups. This is attributed to the increased growth factor expression, such as hepatocyte growth

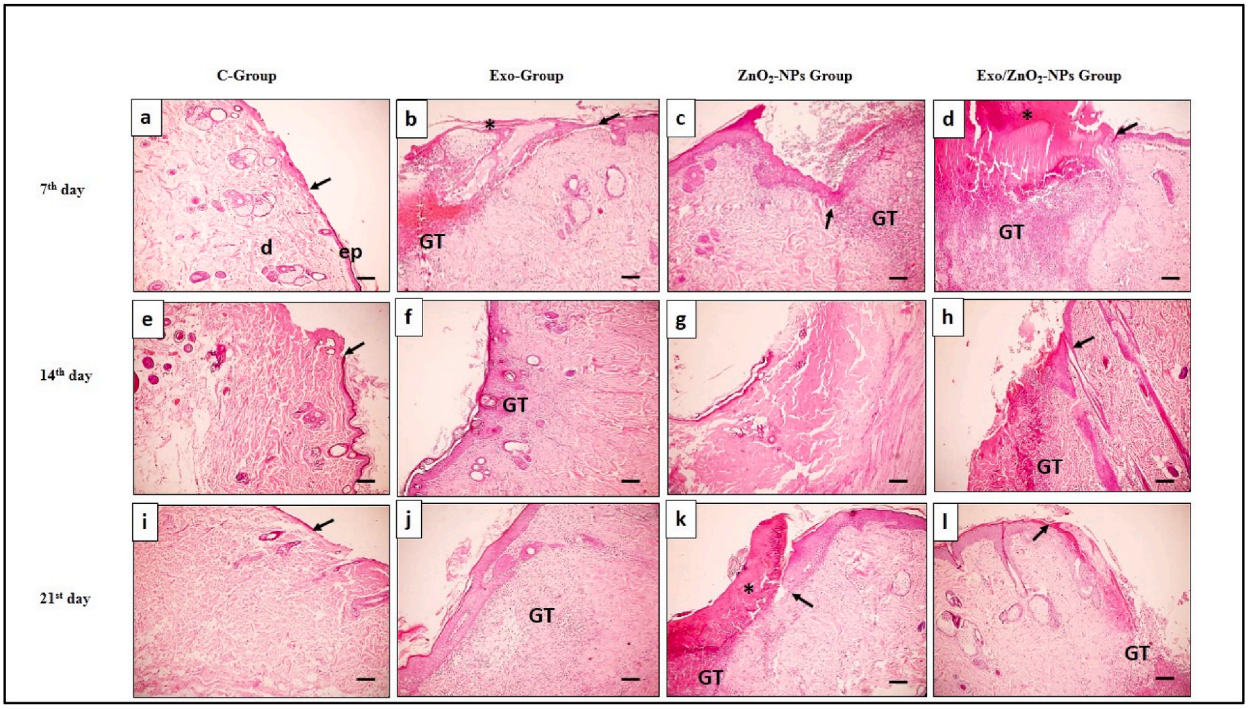

Fig. 7. Photomicrograph of H&E stained sections of wound area in tested groups on days 7, 14, and 21. Control group (C-group) (a, e, i), exosome-treated group (Exo-group) (b, f, j), zinc nanoparticles-treated group (ZnO_2-NPs group) (c, g, k), and Exosome and zinc nanoparticles-treated group (Exo/ZnO_2-NPs group) ((d, h, l). ep = epidermis, d = dermis, GT = granulation tissue, arrow = Wound edge, Asterisk = scab. Scale bars 100 μm.

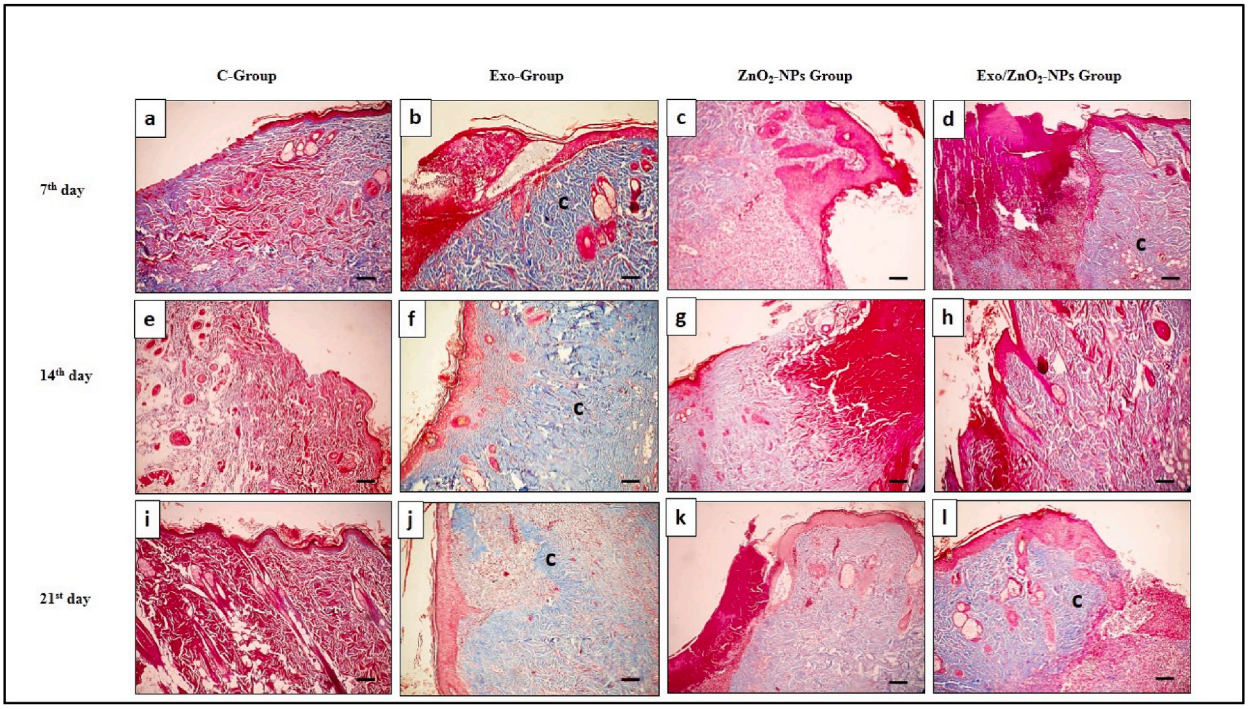

Fig. 8. Masson's trichrome stained sections of wound area in tested groups on days 7, 14, and 21 post-wounding. Control group (C-group) (a, e, i), exosome-treated group (Exo-group) (b, f, j), zinc nanoparticles treated group (ZnO_2-NPs group) (c, g, k), and exosome and zinc nanoparticles treated group (Exo/ZnO_2-NPs group) (d, h, l). Collagen which was stained blue. Scale bars 100 μm. (For interpretation of the references to color in this figure legend, the reader is referred to the Web version of this article.)

factor (HGF), stromal-derived growth factor-1 (SDF1), nerve growth factor (NGF), insulin-like growth factor-1 (IGF1), and cell cycle genes [35]. Growth factors are crucial in regulating the healing process by attracting fibroblasts and inflammatory cells to the wound site and promoting cellular proliferation [36].

The study found that animals in groups treated with ZnO_2-NPs exhibited varying levels of inflammation and tissue necrosis. This finding suggests that ZnO_2-NPs induce cytotoxicity in RGC-5 cells by causing an excessive production of ROS. The excessive production of ROS results in the increased expression of caspase-12, which subsequently causes ER stress. ER, stress then leads to cellular damage and ultimately induces apoptosis or necrosis [37].

Furthermore, stem cell-derived exosomes have been shown to stimulate angiogenesis, which is essential for providing oxygen and nutrients to the healing wound. Exosomes can also influence the remodeling of the extracellular matrix (ECM) at the wound site. They can promote the synthesis and deposition of collagen, enhance the organization of collagen fibers, and regulate the balance between ECM synthesis and degradation [38].

Our results suggested that exosomes significantly decrease GT and scab area. A decrease in granulation tissue during wound healing can indicate progression to the remodeling phase, in which granulation tissue is transient and eventually undergoes remodeling. As the wound healing process advances, the need for granulation tissue decreases, and the tissue begins to transition toward the remodeling phase. During this phase, the focus shifts towards collagen synthesis and organization rather than the presence of granulation tissue. Conversely, the decrease in a scab during wound healing is often associated with the process of re-epithelialization. As the underlying skin cells migrate and proliferate, they gradually cover the wound bed and replace the scab. Previous research suggested that exosomes potentially alleviate scar formation by decreasing the Col1:Col3 ratio [39].

This research also added that the exosome group showed a significant collagen deposition during the three intervals compared to other groups. Collagen deposition is a critical aspect of the wound-healing process. It is the main structural extracellular matrix (ECM) component and provides tissue strength, stability, and integrity. During wound healing, collagen is synthesized and deposited to restore the structural integrity of the injured tissue. Human-induced pluripotent stem cell exosomes can assist in wound healing by stimulating collagen synthesis and maturity [40]**.** Another study [41,42] demonstrated that the transplantation of adipose-derived stem cell exosomes in the wound area stimulated wound healing by promoting collagen deposition through the activation of fibroblast function.

The current study explained a higher expression of α-SMA cells in the exosome group than in other groups during the three intervals. A-SMA is associated with the endothelial cells lining the blood vessels and pericytes. It can contribute to angiogenesis by providing support and guidance to newly forming blood vessels, aiding in the wound-healing process. These findings align with numerous previous studies. One of these studies explained that human embryonic stem cell-derived exosomes accelerate the wound-

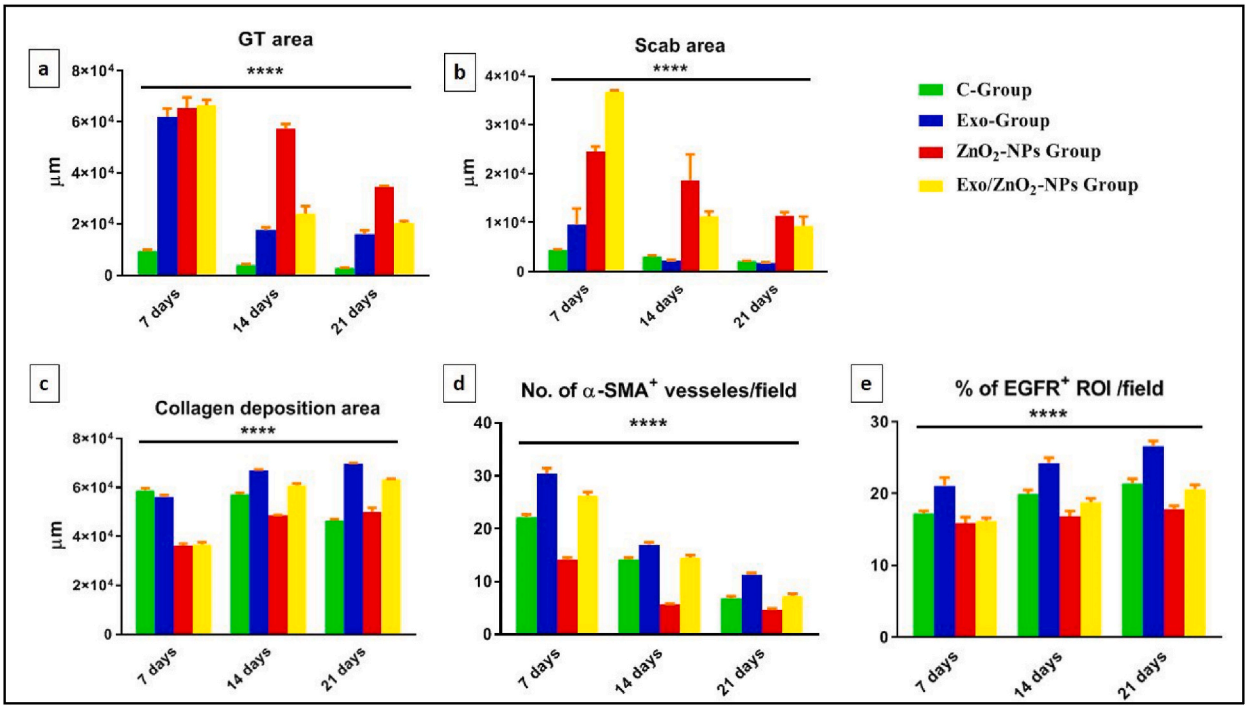

Fig. 9. Different measurements on 7, 14, and 21 days post-wounding between groups; control (C-group), exosome-treated group (Exo-group), zinc nanoparticles treated group (ZNO_2-NPs group), and the combination between exosome and zinc nanoparticles treated group (Exo/ZNO_2-NPs group). GT area (a), scab area (b), collagen deposition area (c), number of alpha-smooth muscle actin (α-SMA) vessels/field (d), and % of epidermal growth factor receptor (EGFR) ROI/field (e). Significant results are represented by asterisks ($p \leq 0.0001$ = ****).

healing process in addition to promoting local angiogenesis at the wound site in aged mice [43]. Another research illustrated that exosomes released from human induced pluripotent stem cells facilitate cutaneous wound healing by promoting new vessel formation and accelerating their maturation in wound sites [40]. Whereas [41], also suggested that transplantation of adipose-derived stem cell exosomes in wound areas stimulated wound healing by promoting angiogenesis by activating the function of vascular endothelial cells.

In contrast, EGFR was significantly increased, especially in the exosome group. It is primarily associated with epithelial cells, and its upregulation can indicate the migration and proliferation of epithelial cells, leading to enhanced re-epithelialization. A study [39] showed that re-epithelialization was accelerated in the exosome-treated mice.

The wound site contains a large number of growth factors [44]. Regulation of growth factors and their varying expression patterns are associated with temporal and spatial characteristics connected to the slow healing of wounds. Substantial alterations in the level of one factor ultimately affect the production of other growth factors and cytokines. For instance, regulation of the growth factor fibroblast growth factor 7 (FGF7) is synthesized by fibroblasts at the site of a wound [45]. Another illustration is the control of the angiogenesis-regulating vascular endothelial growth factor (VEGF), which is produced at the site of a wound by keratinocytes and macrophages [46]. Lysyl oxidase (LOX) is an enzyme that initiates the process of connecting lysine-derived aldehydes, which is essential for the development of collagen, particularly in the healing of wounds [47]. Transforming growth factor-beta 1 (TGF-1) has an outstanding function in wound healing since it is a crucial growth factor modulator of cell proliferation and differentiation [48]. It also contributes to the up-regulation of VEGF [49]. The transcription factor nuclear factor-E2-related factor 2 (Nrf2) modulates several adaptive oxidative stress responses, which are also implicated in differentiation, proliferation, cell migration, and apoptosis [50]. In rat models of diabetic nephropathy, Nrf2 also exhibits therapeutic effects [37]. The gene responsible for promoting apoptosis is referred to as Bcl-2 associated X protein (Bax) and the expression levels of Bax and Bcl-2, which control the bistable characteristics of the apoptotic caspase system, are highly associated with the degree of apoptosis [51].

Furthermore, FGF7, VEGF, LOX, TGFβ1, and Nrf2 genes were significantly upregulated in exosome-treated rats compared to nano zinc and combined Nano zinc exosome groups. However, the BAX gene elicited a contrasting pattern. According to our results, we hypothesized that exosomes facilitate the process of wound healing. There is limited research on the impact of exosomes on wound healing using a gene expression analysis approach [52]. illustrated that exosomes considerably downregulated TNF-α and interleukin (IL)-6 expression. Exosomes also markedly increased phosphorylated AKT and vascular endothelial growth (VEGF) levels in adMSC exosomes. Pervious study [53] discovered that in a rat model with diabetic foot ulcers, exosomes derived from adipose stem cells with elevated Nrf2 gene expression promoted the skin wound healing process by promoting vascularization. Moreover [54], identified transcripts for insulin-like growth factor-1 (IGF-1), glial cell-derived neurotrophic factor (GDNF), brain-derived neurotrophic factor (BDNF), fibroblast growth factor-1 (FGF-1), and NGF.

Neovascularization plays a vital role in keratinocyte survival, newly formed granulation tissue maintenance, and the re-growth of

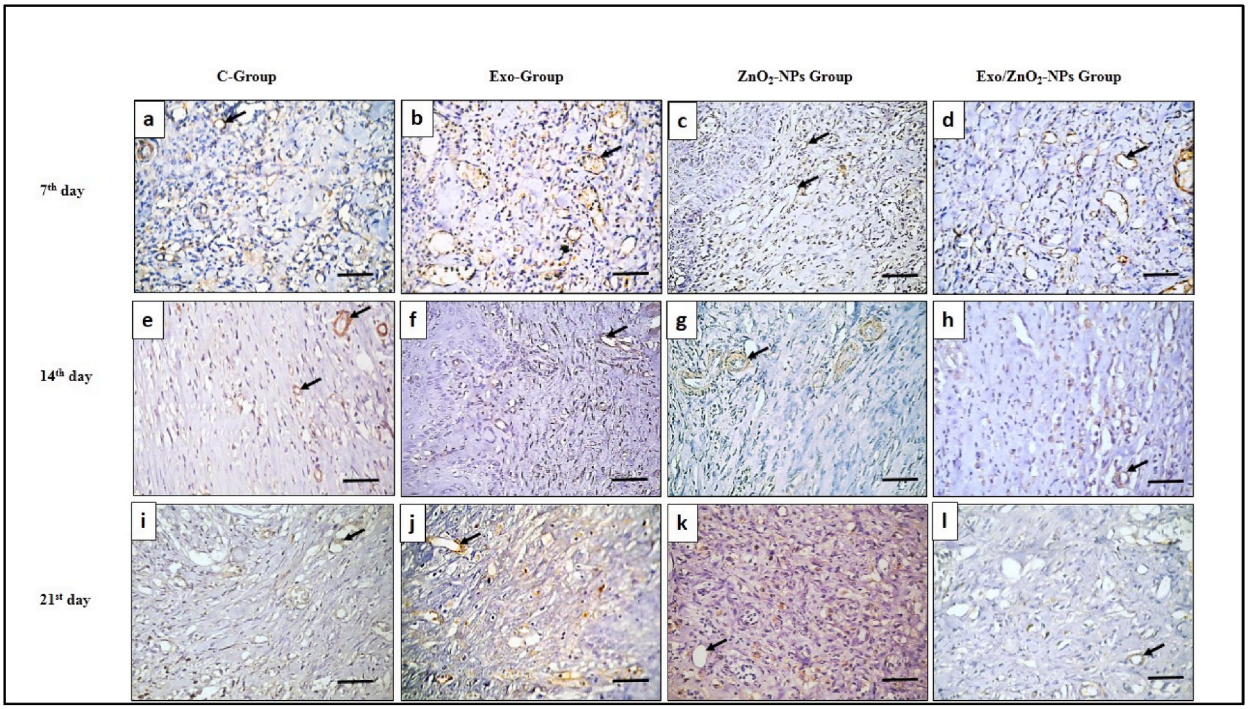

Fig. 10. Immunohistochemically stained sections of wound area against α-SMA marker on days 7, 14, and 21 post-wounding in the control group (C-group) (a, e, i), exosome-treated group (Exo-group) (b, f, j), Zinc nanoparticles treated group (ZnO_2-NPs group) (c, g, k), and Exosome and zinc nanoparticles treated group (Exo/ZnO_2-NPs group) (d, h, l). Positive reacted cells of blood vessels showed a brown color (arrow). Scale bars 50 μm. (For interpretation of the references to color in this figure legend, the reader is referred to the Web version of this article.)

epithelial cells during wound healing [55]. The proliferation and interaction of endothelial cells with angiogenic factors, such as vascular endothelial growth factor and fibroblast growth factor, are essential for the formation of new blood vessels. Exosomes have proven their efficacy in this aspect by effectively enhancing the expression of these angiogenic factors [56]. In addition, they can promote endothelial cell proliferation [35]. Furthermore, it has been shown that stem cell transplantation contributes to wound healing primarily because these cells contain cytokines and growth factors, mRNAs, signaling lipids, and regulatory miRNAs. They are released into the extracellular milieu and play a significant role in intercellular communication [57]. Exosomes carry a variety of molecular components, such as proteins and nucleic acids, which vary depending on the cell or tissue of origin. As a result, they alter the receiving cells' gene expression, controlling cell growth, division, and apoptosis [58]. Inhibiting heat stress-induced apoptosis in keratinocytes by lowering the amount of the pro-apoptotic protein Bax was found to promote cell proliferation after Exosome injection [57]. The aforementioned factors may explain the changes in the gene expression profile of the investigated markers observed in exosome-treated rats.

Our results indicate that both Nano zinc and combined Nano zinc exosome treatments resulted in a decrease in the expression of FGF7, VEGF, LOX, TGFβ1, and Nrf2 genes. Conversely, the BAX gene showed an increase. Our results indicated that nanoparticle zinc hurts the process of wound healing. The impact of nanoparticles on cytotoxicity is markedly affected by their size, shape, and chemical composition [59]. According to Refs. [60,61], the detrimental impact of Nano zinc on the gene expression profile of the genes under study may be related to an unbalanced antioxidant status, cytotoxic effects, and apoptotic death. According to research [62], ZnO_2-NPs caused DNA breakage, increased levels of inflammatory cytokines, apoptotic markers, and heat shock protein-70 in the rat brain after oral exposure. Contrary to our results, nano zinc caused a considerable collagen expression downregulation in skin tissue compared to the lead oxide-impaired group. In comparison to lead oxide skin-exposed rats, co-administration of nano zinc oxide decreased the upregulation of the collagen gene's expression, demonstrating the protective effect of nano zinc oxide cream against lead dermal toxicity [63].

The levels of bioavailable estrogen and testosterone hormones may be affecting wound healing and were not measured is a limitation of this study. Another limitation point was the rats are described as loose-skinned animals [64] because of their skin's redundancy, elasticity, and lack of strong adherence to underlying structures. Thus, rat skin wound healing may not perfectly mimic human skin wound healing due to the differences in skin morphology.

5. Conclusions

Using mesenchymal stem cell exosome-based treatment as a new treatment strategy can improve and accelerate the healing cascade of cutaneous wounds in rats by promoting angiogenesis, re-epithelialization, and collagen deposition. On the other hand, it is crucial to

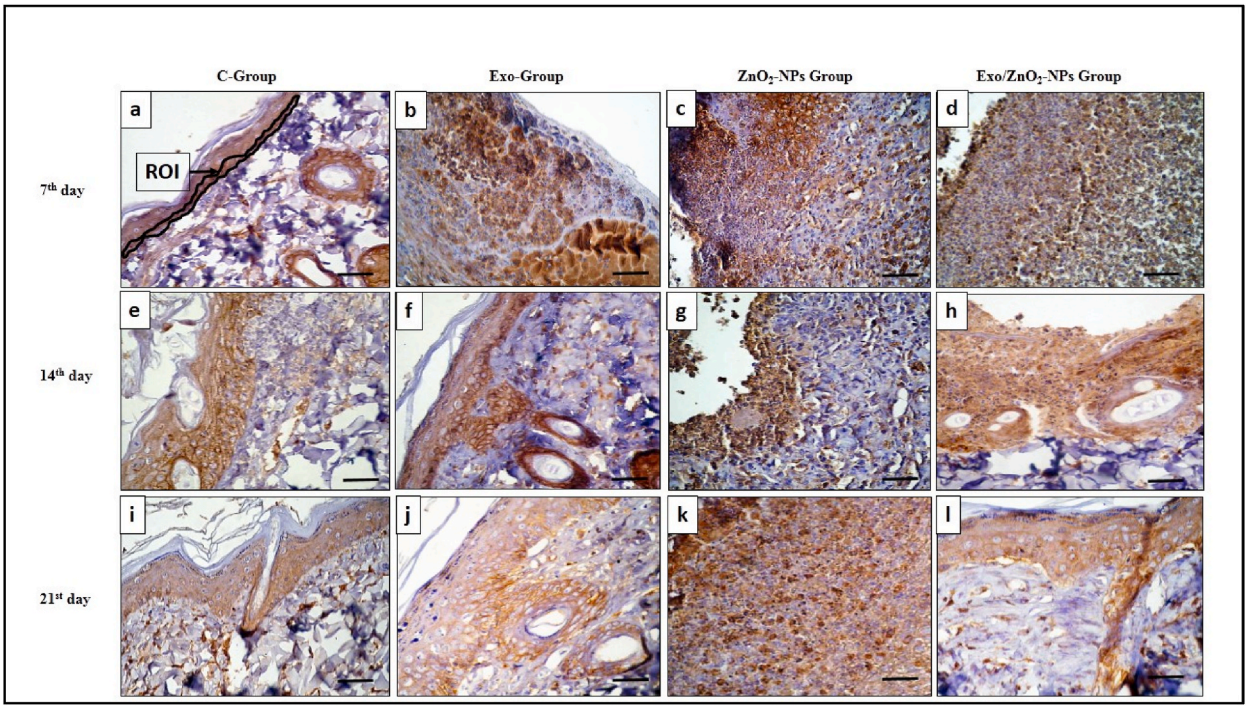

Fig. 11. Immunohistochemically stained sections of wound area against EGFR marker on days 7, 14, and 21 post-wounding in the control group (C-group) (a, e, i), exosome-treated group (Exo-group) (b, f, j), zinc nanoparticles treated group (ZnO_2-NPs group) (c, g, k), and exosome and zinc nanoparticles treated group (Exo/ZnO_2-NPs group) (d, h, l). Region of interest (ROI) showed a brown reaction among epithelial cells. Scale bars 50 μm. (For interpretation of the references to color in this figure legend, the reader is referred to the Web version of this article.)

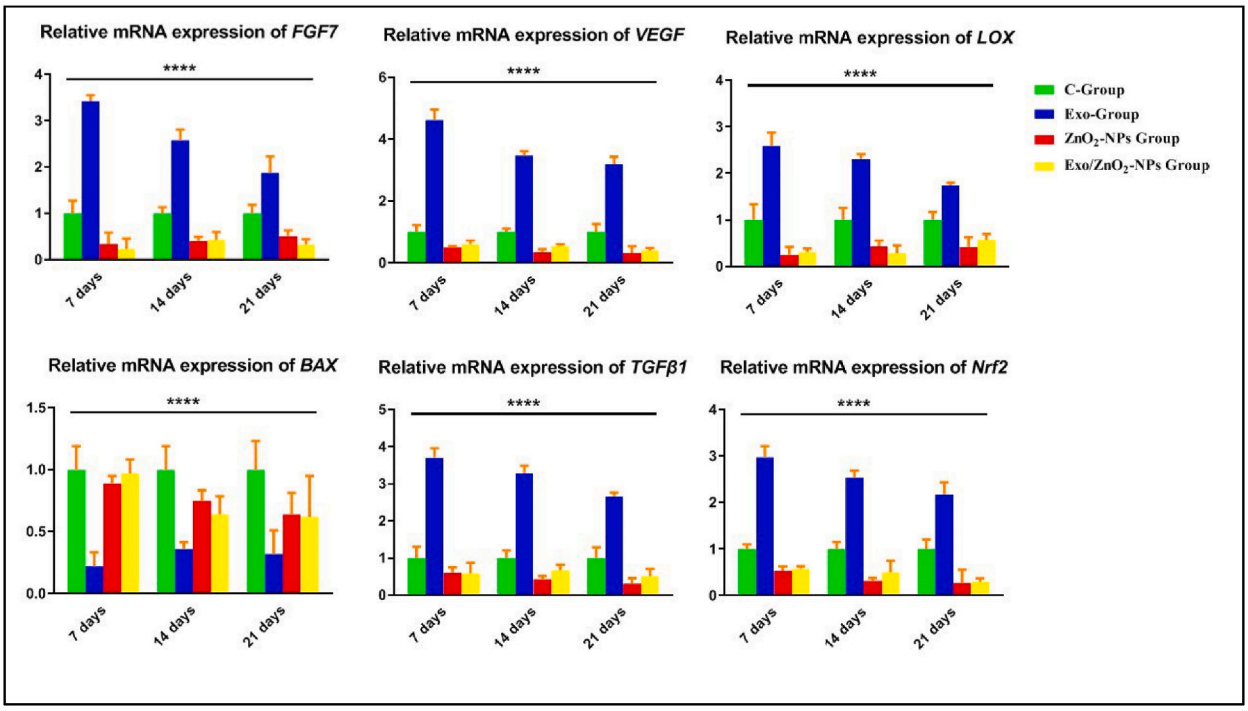

Fig. 12. The relative expression of FGF7, VEGF, LOX, BAX, TGFβ1, and Nrf2 mRNA among treated groups; the control group (C-group), exosome-treated group (Exo-group), Zinc nanoparticles treated group (ZNO_2-NPs group) and the combination between exosome and zinc nanoparticles treated group (Exo/ZNO_2-NPs group) at 7th, 14th, and 21st days post-wounding.

establish a consensus regarding the definition and standardization of variables related to exosome preparation, quantification, administration, and evaluation. Further studies are needed to explain the technical challenges associated with exosomes and to how they can be applied in practical clinical cases.

Ethics approval and consent to participate

All animal experiments were approved by the Mansoura University Animal Care and Use Committee (MU-ACUC) with the code number VM.R.24.10.181 and were conducted in accordance with the guidelines of the Animal Care and Use Committee of Mansoura University.

Author disclosure statement

No competing financial interests exist.

Funding

Open Access funding enabled and organized by Projekt DEAL. This work was supported by the University of Witten-Herdecke Germany.

Data availability statement

This article contains all data generated or analyzed throughout this research. The data supporting the study's findings are available from the author upon reasonable request.

CRediT authorship contribution statement

Mohamed Salem: Methodology, Investigation, Conceptualization. **Ahmed Ateya:** Methodology, Conceptualization. **Zeinab Shouman:** Writing – original draft, Methodology, Investigation, Conceptualization. **Basma Salama:** Methodology, Investigation, Conceptualization. **Basma Hamed:** Visualization, Investigation. **Gaber Batiha:** Writing – original draft, Methodology, Conceptualization. **Farid Ataya:** Writing – review & editing, Methodology, Funding acquisition, Conceptualization. **Athanasios Alexiou:** Supervision. **Marios Papadakis:** Writing – review & editing, Writing – original draft, Supervision. **Marwa Abass:** Writing – review & editing, Supervision, Methodology, Data curation, Conceptualization.

Declaration of competing interest

The authors declare that they have no known competing financial interests or personal relationships that could have appeared to influence the work reported in this paper.

Acknowledgments

The authors would like to extend their gratitude to King Saud University (Riyadh, Saudi Arabia) for funding this research through Researchers supporting Project number (RSPD2024R693).

Abbreviations

BM	Bone marrow
PBS	Phosphate-buffered saline.
BM-MSCs	Bone Marrow- Mesenchymal Stem Cells
ZnO_2-NPs	Zinc Oxide nanoparticles
TEM	Transmission electron microscope
EDX	The Energy Dispersive X-ray
α-SMA	alpha-smooth muscle actin
EGFR	epidermal growth factor receptor
Nrf2 mRNA	The relative renal nuclear factor erythroid 2-related factor2
TGFβ1	Transforming growth factor beta-1
FGF7	Fibroblast growth factor-7
TGFβ1	Transforming growth factor beta-1
LOX	Lysyl oxidase
VEGF	Vascular endothelial growth factor

References

[1] F. Öztürk, A.T. Ermertcan, Wound healing: a new approach to the topical wound care, Cutan. Ocul. Toxicol. 30 (2011) 92–99, https://doi.org/10.3109/15569527.2010.539586.
[2] J.G. Powers, C. Higham, K. Broussard, T.J. Phillips, Wound healing and treating wounds: chronic wound care and management, J. Am. Acad. Dermatol. 74 (2016) 607–625, https://doi.org/10.1016/j.jaad.2015.08.070.
[3] J. Reinke, H. Sorg, Wound repair and regeneration, Eur. Surg. Res. 49 (2012) 35–43, https://doi.org/10.1159/000339613.
[4] S. Naraginti, P.L. Kumari, R.K. Das, A. Sivakumar, S.H. Patil, V.V. Andhalkar, Amelioration of excision wounds by topical application of green synthesized, formulated silver and gold nanoparticles in albino Wistar rats, Mater. Sci. Eng. C 62 (2016) 293–300, https://doi.org/10.1016/j.msec.2016.01.069.
[5] A.Y. Koga, B. Carletto, P.V. Farago, L.C. Lipinski, Evaluation of cutaneous wound healing effect of associated zinc oxide (ZnO) and estrogen (E2) nanoparticles, Braz. J. Dev. 7 (2021) 32382–32393, https://doi.org/10.34117/bjdv7n3-790.
[6] M. Moniri, A. Boroumand Moghaddam, S. Azizi, R. Abdul Rahim, W. Zuhainis Saad, M. Navaderi, P. Arulselvan, R. Mohamad, Molecular study of wound healing after using biosynthesized BNC/Fe3O4 nanocomposites assisted with a bioinformatics approach, Int. J. Nanomedicine (2018) 2955–2971, https://doi.org/10.2147/IJN.S159637.
[7] S. Kantipudi, J.R. Sunkara, M. Rallabhandi, C.V. Thonangi, R.D. Cholla, P. Kollu, M.K. Parvathaneni, S.V.N. Pammi, Enhanced wound healing activity of Ag–ZnO composite NPs in Wistar Albino rats, IET Nanobiotechnol. 12 (2018) 473–478, https://doi.org/10.1049/iet-nbt.2017.0087.
[8] A. Kołodziejczak-Radzimska, T. Jesionowski, Zinc oxide—from synthesis to application: a review, Materials 7 (2014) 2833–2881, https://doi.org/10.3390/ma7042833.
[9] P.K. Mishra, H. Mishra, A. Ekielski, S. Talegaonkar, B. Vaidya, Zinc oxide nanoparticles: a promising nanomaterial for biomedical applications, Drug Discov. Today 22 (2017) 1825–1834, https://doi.org/10.1016/j.drudis.2017.08.006.
[10] W. Ko, N. Jung, M. Lee, M. Yun, S. Jeon, Electronic nose based on multipatterns of ZnO nanorods on a quartz resonator with remote electrodes, ACS Nano 7 (2013) 6685–6690, https://doi.org/10.1021/nn4027245.
[11] Y. Zhang, T. R Nayak, H. Hong, W. Cai, Biomedical applications of zinc oxide nanomaterials, Curr. Mol. Med. 13 (2013) 1633–1645.
[12] E. Yadav, D. Singh, P. Yadav, A. Verma, Ameliorative effect of biofabricated ZnO nanoparticles of Trianthema portulacastrum Linn. on dermal wounds via removal of oxidative stress and inflammation, RSC Adv. 8 (2018) 21621–21635, https://doi.org/10.1039/C8RA03500H.
[13] R. Raguvaran, B.K. Manuja, M. Chopra, R. Thakur, T. Anand, A. Kalia, A. Manuja, Sodium alginate and gum acacia hydrogels of ZnO nanoparticles show wound healing effect on fibroblast cells, Int. J. Biol. Macromol. 96 (2017) 185–191, https://doi.org/10.1016/j.ijbiomac.2016.12.009.
[14] R. Kalluri, V.S. LeBleu, The biology, function, and biomedical applications of exosomes, Science 367 (2020) eaau6977, https://doi.org/10.1126/science.aau6977.
[15] D.G. Phinney, M.F. Pittenger, Concise review: MSC-derived exosomes for cell-free therapy, Stem Cell. 35 (2017) 851–858, https://doi.org/10.1002/stem.2575.
[16] Y. Song, Z. Li, T. He, M. Qu, L. Jiang, W. Li, X. Shi, J. Pan, L. Zhang, Y. Wang, M2 microglia-derived exosomes protect the mouse brain from ischemia-reperfusion injury via exosomal miR-124, Theranostics 9 (2019) 2910, https://doi.org/10.7150/thno.30879.
[17] R. Wu, W. Gao, K. Yao, J. Ge, Roles of exosomes derived from immune cells in cardiovascular diseases, Front. Immunol. 10 (2019) 648, https://doi.org/10.3389/fimmu.2019.00648.
[18] Y. Ge, W. Mu, Q. Ba, J. Li, Y. Jiang, Q. Xia, H. Wang, Hepatocellular carcinoma-derived exosomes in organotropic metastasis, recurrence and early diagnosis application, Cancer Lett. 477 (2020) 41–48, https://doi.org/10.1016/j.canlet.2020.02.003.
[19] J. Xu, S. Bai, Y. Cao, L. Liu, Y. Fang, J. Du, L. Luo, M. Chen, B. Shen, Q. Zhang, miRNA-221-3p in endothelial progenitor cell-derived exosomes accelerates skin wound healing in diabetic mice, Diabetes Metab. Syndr. Obes. (2020) 1259–1270, https://doi.org/10.2147/DMSO.S243549.
[20] J. Wang, H. Wu, Y. Peng, Y. Zhao, Y. Qin, Y. Zhang, Z. Xiao, Hypoxia adipose stem cell-derived exosomes promote high-quality healing of diabetic wound involves activation of PI3K/Akt pathways, J. Nanobiotechnology 19 (2021) 1–13, https://doi.org/10.1186/s12951-021-00942-0.
[21] D. Ti, H. Hao, C. Tong, J. Liu, L. Dong, J. Zheng, Y. Zhao, H. Liu, X. Fu, W. Han, LPS-preconditioned mesenchymal stromal cells modify macrophage polarization for resolution of chronic inflammation via exosome-shuttled let-7b, J. Transl. Med. 13 (2015) 1–14, https://doi.org/10.1186/s12967-015-0642-6.
[22] Y. Xiong, L. Chen, C. Yan, W. Zhou, Y. Endo, J. Liu, L. Hu, Y. Hu, B. Mi, G. Liu, Circulating exosomal miR-20b-5p inhibition restores Wnt9b signaling and reverses diabetes-associated impaired wound healing, Small 16 (2020) 1904044, https://doi.org/10.1002/smll.201904044.
[23] C. Kilkenny, D. Altman, Improving bioscience research reporting: ARRIVE-ing at a solution, Lab. Anim. 44 (2010) 377–378, https://doi.org/10.1371/journal.pbio.1000412.
[24] X. Wang, Z. Li, Y. Cui, X. Cui, C. Chen, Z. Wang, Exosomes isolated from bone marrow mesenchymal stem cells exert a protective effect on osteoarthritis via lncRNA LYRM4-AS1-GRPR-miR-6515-5p, Front. Cell Dev. Biol. 9 (2021) 644380, https://doi.org/10.3389/fcell.2021.644380.
[25] N. Yusop, P. Battersby, A. Alraies, A.J. Sloan, R. Moseley, R.J. Waddington, Isolation and characterisation of mesenchymal stem cells from rat bone marrow and the endosteal niche: a comparative study, Stem Cells Int. 2018 (2018), https://doi.org/10.1155/2018/6869128.
[26] G.A. Fielding, A. Bandyopadhyay, S. Bose, Effects of silica and zinc oxide doping on mechanical and biological properties of 3D printed tricalcium phosphate tissue engineering scaffolds, Dent. Mater. 28 (2012) 113–122, https://doi.org/10.1016/j.dental.2011.09.010.
[27] G.S. Doig, F. Simpson, Randomization and allocation concealment: a practical guide for researchers, J. Crit. Care 20 (2005) 187–191, https://doi.org/10.1016/j.jcrc.2005.04.005.
[28] M.M. Sperry, Y.-H. Yu, R.L. Welch, E.J. Granquist, B.A. Winkelstein, Grading facial expression is a sensitive means to detect grimace differences in orofacial pain in a rat model, Sci. Rep. 8 (2018) 13894, https://doi.org/10.1038/s41598-018-32297-2.
[29] D. Dwivedi, M. Dwivedi, S. Malviya, V. Singh, Evaluation of wound healing, anti-microbial and antioxidant potential of Pongamia pinnata in wistar rats, J. Tradit. Complement. Med. 7 (2017) 79–85, https://doi.org/10.1016/j.jtcme.2015.12.0022.
[30] G. Anderson, J. Bancroft, Tissue processing and microtomy, Theory Pract. Histol. Tech. 5 (2002) 85–99.
[31] M.H. Flint, M.F. Lyons, M. Meaney, D. Williams, The Masson staining of collagen—an explanation of an apparent paradox, Histochem. J. 7 (1975) 529–546, https://doi.org/10.1007/BF01003791.
[32] S.-W. Kim, J. Roh, C.-S. Park, Immunohistochemistry for pathologists: protocols, pitfalls, and tips, J. Pathol. Transl, Med. 50 (2016) 411, https://doi.org/10.4132/jptm.2016.08.08.
[33] L.R. de Moura Estevão, P. Cassini-Vieira, A.G.B. Leite, A.A.V. de Carvalho Bulhões, L. da Silva Barcelos, J. Evêncio-Neto, Morphological evaluation of wound healing events in the excisional wound healing model in rats, Bio-Protoc 9 (2019) e3285, https://doi.org/10.21769/BioProtoc.3285, e3285.
[34] M.W. Pfaffl, A new mathematical model for relative quantification in real-time RT–PCR, Nucleic Acids Res. 29 (2001) e45, https://doi.org/10.1093/nar/29.9.e45, e45.
[35] A. Shabbir, A. Cox, L. Rodriguez-Menocal, M. Salgado, E.V. Badiavas, Mesenchymal stem cell exosomes induce proliferation and migration of normal and chronic wound fibroblasts, and enhance angiogenesis in vitro, Stem Cells Dev. 24 (2015) 1635–1647, https://doi.org/10.1089/scd.2014.0316.
[36] H. Sorg, D.J. Tilkorn, S. Hager, J. Hauser, U. Mirastschijski, Skin wound healing: an update on the current knowledge and concepts, Eur. Surg. Res. 58 (2017) 81–94, https://doi.org/10.1159/000454919.
[37] D. Guo, H. Bi, B. Liu, Q. Wu, D. Wang, Y. Cui, Reactive oxygen species-induced cytotoxic effects of zinc oxide nanoparticles in rat retinal ganglion cells, Toxicol. Vitro 27 (2013) 731–738, https://doi.org/10.1016/j.tiv.2012.12.001.
[38] M.D. Hade, C.N. Suire, Z. Suo, Mesenchymal stem cell-derived exosomes: applications in regenerative medicine, Cells 10 (2021) 1959, https://doi.org/10.3390/cells10081959.
[39] R. Dalirfardouei, K. Jamialahmadi, A.H. Jafarian, E. Mahdipour, Promising effects of exosomes isolated from menstrual blood-derived mesenchymal stem cell on wound-healing process in diabetic mouse model, J. Tissue Eng. Regen. Med. 13 (2019) 555–568, https://doi.org/10.1002/term.2799.
[40] H. Zheng, S.A. Whitman, W. Wu, G.T. Wondrak, P.K. Wong, D. Fang, D.D. Zhang, Therapeutic potential of Nrf2 activators in streptozotocin-induced diabetic nephropathy, Diabetes 60 (2011) 3055–3066, https://doi.org/10.2337/db11-0807.

[41] H. Yu, Y. Wu, B. Zhang, M. Xiong, Y. Yi, Q. Zhang, M. Wu, Exosomes derived from E2F1–/–adipose-derived stem cells promote skin wound healing via miR-130b-5p/TGFBR3 Axis, Int. J. Nanomedicine (2023) 6275–6292, https://doi.org/10.2147/IJN.S431725.
[42] J. Yang, Z. Wang, X. Liang, W. Wang, S. Wang, Multifunctional polypeptide-based hydrogel bio-adhesives with pro-healing activities and their working principles, Adv. Colloid Interface Sci. (2024) 103155.
[43] B. Chen, Y. Sun, J. Zhang, Q. Zhu, Y. Yang, X. Niu, Z. Deng, Q. Li, Y. Wang, Human embryonic stem cell-derived exosomes promote pressure ulcer healing in aged mice by rejuvenating senescent endothelial cells, Stem Cell Res. Ther. 10 (2019) 1–17, https://doi.org/10.1186/s13287-019-1253-6.
[44] S. Dogan, S. Demirer, I. Kepenekci, B. Erkek, A. Kiziltay, N. Hasirci, S. Müftüoğlu, A. Nazikoğlu, N. Renda, U. Dincer, Epidermal growth factor-containing wound closure enhances wound healing in non-diabetic and diabetic rats, Int. Wound J. 6 (2009) 107–115, https://doi.org/10.1111/j.1742-481X.2009.00584.x.
[45] E.C.D.J.D. Masi, A.C.L. Campos, F.D.J.D. Masi, M.A.S. Ratti, I. Shin Ike, R.D.J.D. Masi, A influência de fatores de crescimento na cicatrização de feridas cutâneas de ratas, Braz. J. Otorhinolaryngol. 82 (2016) 512–521, https://doi.org/10.1016/j.bjorl.2015.09.011.
[46] Z. Xie, C.B. Paras, H. Weng, P. Punnakitikashem, L.-C. Su, K. Vu, L. Tang, J. Yang, K.T. Nguyen, Dual growth factor releasing multi-functional nanofibers for wound healing, Acta Biomater. 9 (2013) 9351–9359, https://doi.org/10.1016/j.actbio.2013.07.030.
[47] H. Fushida-Takemura, M. Fukuda, N. Maekawa, M. Chanoki, H. Kobayashi, N. Yashiro, M. Ishii, T. Hamada, S. Otani, A. Ooshima, Detection of lysyl oxidase gene expression in rat skin during wound healing, Arch. Dermatol. Res. 288 (1996) 7–10, https://doi.org/10.1007/BF02505035.
[48] H. El Gazaerly, D.M. Elbardisey, H.M. Eltokhy, D. Teaama, Effect of transforming growth factor Beta 1 on wound healing in induced diabetic rats, Int. J. Health Sci. 7 (2013) 160, https://doi.org/10.12816/0006040.
[49] H. Du, D. Jiang, G. Song, C. Cao, D. Zhang, P. Yu, C. Lai, X. Guo, X. Zong, X. Jin, Wound healing activity of phage-sisplayed TGF-β1 model peptide in streptozotocin-Induced diabetic rats, Int. J. Pept. Res. Ther. 27 (2021) 1079–1094, https://doi.org/10.1007/s10989-020-10152-1.
[50] Y. Lee, J.-M. Shin, S. Jang, D.-K. Choi, M.-S. Seo, H.-R. Kim, K.-C. Sohn, M. Im, Y.-J. Seo, J.-H. Lee, Role of nuclear factor E2-related factor 2 (Nrf2) in epidermal differentiation, Arch. Dermatol. Res. 306 (2014) 677–682, https://doi.org/10.1007/s00403-014-1470-x.
[51] Y. Cui, G. Xia, X. Fu, H. Yang, R. Peng, Y. Zhang, Q. Gu, Y. Gao, X. Cui, W. Hu, Relationship between expression of Bax and Bcl-2 proteins and apoptosis in radiation compound wound healing of rats, Chin. J. Traumatol. Zhonghua Chuang Shang Za Zhi 6 (2003) 135–138.
[52] M. Li, T. Wang, H. Tian, G. Wei, L. Zhao, Y. Shi, Macrophage-derived exosomes accelerate wound healing through their anti-inflammation effects in a diabetic rat model, Artif, Cells Nanomedicine Biotechnol. 47 (2019) 3793–3803, https://doi.org/10.1080/21691401.2019.1669617.
[53] X. Li, X. Xie, W. Lian, R. Shi, S. Han, H. Zhang, L. Lu, M. Li, Exosomes from adipose-derived stem cells overexpressing Nrf2 accelerate cutaneous wound healing by promoting vascularization in a diabetic foot ulcer rat model, Exp. Mol. Med. 50 (2018) 1–14, https://doi.org/10.1038/s12276-018-0058-5.
[54] V. Bucan, D. Vaslaitis, C.-T. Peck, S. Strauß, P.M. Vogt, C. Radtke, Effect of exosomes from rat adipose-derived mesenchymal stem cells on neurite outgrowth and sciatic nerve regeneration after crush injury, Mol. Neurobiol. 56 (2019) 1812–1824, https://doi.org/10.1007/s12035-018-1172-z.
[55] T. de Mayo, P. Conget, S. Becerra-Bayona, C.L. Sossa, V. Galvis, M.L. Arango-Rodríguez, The role of bone marrow mesenchymal stromal cell derivatives in skin wound healing in diabetic mice, PLoS One 12 (2017) e0177533, https://doi.org/10.1371/journal.pone.0177533.
[56] U.T.T. Than, D. Guanzon, D. Leavesley, T. Parker, Association of extracellular membrane vesicles with cutaneous wound healing, Int. J. Mol. Sci. 18 (2017) 956, https://doi.org/10.3390/ijms18050956.
[57] J. Zhang, J. Guan, X. Niu, G. Hu, S. Guo, Q. Li, Z. Xie, C. Zhang, Y. Wang, Exosomes released from human induced pluripotent stem cells-derived MSCs facilitate cutaneous wound healing by promoting collagen synthesis and angiogenesis, J. Transl. Med. 13 (2015) 1–14, https://doi.org/10.1186/s12967-015-0417-0.
[58] S. Inamdar, R. Nitiyanandan, K. Rege, Emerging applications of exosomes in cancer therapeutics and diagnostics, Bioengineering & Translational Medicine 2 (2017) 70–80, n.d.
[59] N. Talebian, H.S.H. Zavvare, Enhanced bactericidal action of SnO2 nanostructures having different morphologies under visible light: influence of surfactant, J. Photochem. Photobiol., B 130 (2014) 132–139, https://doi.org/10.1016/j.jphotobiol.2013.10.018.
[60] H. Papavlassopoulos, Y.K. Mishra, S. Kaps, I. Paulowicz, R. Abdelaziz, M. Elbahri, E. Maser, R. Adelung, C. Röhl, Toxicity of functional nano-micro zinc oxide tetrapods: impact of cell culture conditions, cellular age and material properties, PLoS One 9 (2014) e84983, https://doi.org/10.1371/journal.pone.0084983.
[61] F. Xiaoli, W. Junrong, L. Xuan, Z. Yanli, W. Limin, L. Jia, S. Longquan, Prenatal exposure to nanosized zinc oxide in rats: neurotoxicity and postnatal impaired learning and memory ability, Nanomed 12 (2017) 777–795, https://doi.org/10.2217/nnm-2016-0397.
[62] H. Attia, H. Nounou, M. Shalaby, Zinc oxide nanoparticles induced oxidative DNA damage, inflammation and apoptosis in rat's brain after oral exposure, Toxics 6 (2018) 29, https://doi.org/10.3390/toxics6020029.
[63] A. Khalaf, E.I. Hassanen, R.A. Azouz, A.R. Zaki, M.A. Ibrahim, K.Y. Farroh, M.K. Galal, Ameliorative effect of zinc oxide nanoparticles against dermal toxicity induced by lead oxide in rats, Int. J. Nanomedicine (2019) 7729–7741, https://doi.org/10.2147/ijn.s220572.
[64] W.A. Dorsett-Martin, Rat models of skin wound healing: a review, Wound Repair Regen. 12 (2004) 591–599, https://doi.org/10.1111/j.1067-1927.2004.12601.x.